Deregulation of desmosomal proteins and extracellular matrix proteases in odontogenic keratocyst

Marina Gonçalves Diniz[1,*], Filipe Fideles Duarte-Andrade[2], Fernanda Stussi[3],
Jéssica Gardone Vitório[2], Felipe Paiva Fonseca[2,4], Romênia Ramos Domingues[5],
Adriana F. Paes Leme[5], Carolina Cavaliéri Gomes[1], Ricardo Santiago Gomez[2]

[1]Department of Pathology, Biological Sciences Institute, Universidade Federal de Minas Gerais (UFMG), Belo Horizonte, Brazil
[2]Department of Oral Surgery and Pathology, School of Dentistry, Universidade Federal de
Minas Gerais (UFMG), Belo Horizonte, Brazil [3]Department of Biochemistry and Immunology, Biological Sciences Institute, Universidade Federal de Minas Gerais, Belo Horizonte, Brazil
[4]Department of Oral Pathology and Oral Biology, School of Dentistry, University of
Pretoria, Pretoria, South Africa
[5]Laboratório de Espectrometria de Massas, Laboratório Nacional de Biociências (LNBio),
Centro Nacional de Pesquisa em Energia e Materiais (CNPEM), Campinas, Brazil

*Correspondence: Marina Gonçalves Diniz, Department of Pathology, Biological Sciences Institute,
Universidade Federal de Minas Gerais (UFMG). Av. Presidente Antônio Carlos,
6627 - Pampulha, Belo Horizonte, MG CEP: 31270-901, Brazil.
Email: mgdiniz@ufmg.br

ABSTRACT

Objective: Odontogenic keratocyst (OKC) is a benign lesion that tends to recur after surgical treatment. In an attempt to clarify the molecular basis underlining the OKC pathobiology, we aimed to analyze its proteomic profile.

Materials and Methods: We compared the proteomic profiles of five OKC and matched normal oral mucosa by using liquid chromatography–tandem mass spectrometry (LC-MS/MS). Then, we performed enrichment analysis and a literature search for the immunoexpression of the proteomics targets.

Results: We identified 1,150 proteins and 72 differently expressed proteins (log2 fold change $\geq$ 1.5; $p <$ .05). Twenty-seven peptides were exclusively detected in the OKC samples. We found 35 enriched pathways related to cell differentiation and tissue architecture, including keratinocyte differentiation, keratinization, desmosome, and extracellular matrix (ECM) organization and degradation. The immunoexpression information of 11 out of 50 proteins identified in the enriched pathways was obtained. We found the downregulation of four desmosomal proteins (*JUP, PKP1*, *PKP3*, and *PPL*) and upregulation of ECM proteases (MMP-2, MMP-9, and cathepsins).

Conclusions: Proteomic analysis strengthened the notion that OKC cells have a similar proteomic profile to oral keratinocytes. Contextual investigation of the differentially expressed proteins revealed the deregulation of desmosome proteins and ECM degradation as important alterations in OKC pathobiology.

Keywords: desmosomes, matrix metallopoteinases, odontogenic keratocyst, odontogenic tumor, proteome

1 INTRODUCTION

Odontogenic keratocyst (OKC) is a cystic lesion showing a cavity lined with corrugated parakeratinized epithelium, with keratin in the lumen. The epithelium has a well-defined basal cell layer composed of cuboidal or columnar cells with polarized nuclei and a scant spinous cell layer. The capsule wall is composed of fibrous or dense connective tissue where "daughter" cysts may be present (Odell, 2017).

The OKC is an unusual cyst compared to other jaw cysts. While most epithelial cysts are thought to grow passively driven by hydrostatic pressure inside the lumen, OKC is believed to grow as a result of active cellular proliferation (Odell, 2017). In addition, OKC might be associated with the nevoid basal cell carcinoma syndrome and present a high recurrence rate (El-Naggar, Chan, Grandis, Takata, & Slootweg, 2017). The unique nature of OKC is reflected by the difficulties with its classification. In 2005, the World Health Organization/ (WHO) Classification of Head and Neck Tumors edition classified OKC as a tumor and named it "keratocystic odontogenic tumor" (Barnes, Eveson, Reichard, & Sidransky, 2005). In 2017, it was brought back under the heading of cysts (El-Naggar et al., 2017).

The main molecular alterations reported in OKC are the *PTCH1* mutation and the constitutive activation of the Shh cell signaling pathway (Gomes, Guimarães, Diniz, & Gomez, 2017). However, *PTCH1* alterations are also seen in other jaw cysts, such as dentigerous cysts and orthokeratinized odontogenic cyst (Diniz, Galvão, Macedo, Gomes, & Gomez, 2011; Pavelić et al., 2001). Of note, in *PTCH1*-negative OKC cases, the underlining molecular alteration remains obscure (Qu et al., 2019).

The transcriptome analysis of OKC showed the overexpression of genes associated with squamous epithelium and indicated differentiation toward keratinocytes (Heikinheimo et al., 2015). Interesting, after OKC decompression or marsupialization, the OKC lining resembles, histologically, keratinocytes of the normal oral mucosa. Some authors suggested that OKC may originate from the oral epithelium (Ide et al., 2010). In the present study, we aimed to analyze the biological function of expressed proteins (proteome) of OKC and the matched oral mucosa in an attempt to clarify the molecular basis underlining the pathobiology of the OKC.

2 MATERIAL AND METHODS

2.1 Samples and subjects

The study was approved by the institutional review board and the Ethics Committee of Universidade Federal de Minas Gerais (28278620.2.0000.5149) and was conducted in full

accordance with ethical principles, including the World Medical Association Declaration of Helsinki (version 2002). Five fresh tissue samples of OKC and adjacent normal oral mucosa of the five subjects were obtained. Four cases were sporadic, and one was associated with Gorlin–Goltz syndrome. The male/female ratio was 3:2, and ages ranged from 13 to 53 years (median = 34.2). A fragment of the tissue was collected during the excisional biopsy, submerged in RNAlater solution (Ambion Life Technologies), and stored in liquid nitrogen until use. The hematoxylin and eosin (HE) slides were revised to confirm the final diagnosis. Experiments were undertaken with the understanding and written consent of each subject and according to the above mentioned principles.

2.2 Protein isolation and digestion

Samples were homogenized with 1 ml TRIzol (ThermoFischer), and extraction was performed according to manufacturer's instructions. Proteins were precipitated using chloroform/methanol, resuspended in 8 M urea and dissolved by pipetting and sonication in an ultrasonic bath. Protein extracts were quantified by Bradford assay (Biorad).

Proteins were reduced using 10 mM dithiothreitol for 25 min at 56°C and alkylated with 28 mM iodoacetamide for 30 min at room temperature (in the dark). The remaining iodoacetamide was quenched by the addition of 10 mM dithiothreitol for 15 min at room temperature. Then, the urea concentration of the solution was diluted to a final concentration of 1.6 M with 50 mM ammonium bicarbonate. Protein digestion was performed during 16 hr at 37°C by adding sequencing grade-modified trypsin (1:50 enzyme: substrate ratio) (Promega). The reaction was quenched with 0.4% trifluoroacetic acid, and the tryptic digests were desalted with C18 stage tips (Rappsilber, Mann, & Ishihama, 2007), dried in a vacuum concentrator, reconstituted in 0.1% formic acid, and stored at − 20°C for subsequent analysis by liquid chromatography–tandem mass spectrometry (LC-MS/MS).

2.3 Liquid chromatography–tandem mass spectrometry analysis

Peptides were analyzed in LTQ OrbitrapVelos mass spectrometer (ThermoFisher) coupled to EASY-nLC nanoflow liquid chromatography system (ProxeonBiosystem) using a Proxeon nanoelectrospray ion source. Peptides were separated on a PicoFrit (New Objective) column using a gradient of 2%–90% acetonitrile in 0.1% formic acid and a constant flow of 300 nl/min for 80 min. The nanoelectrospray voltage was set to 2.2 kV, and the source temperature was set to 275°C. LTQ Orbitrab Velos was operated in Data Dependent Acquisition (DDA) mode. The (MS1) spectra were acquired on the Orbitrap analyzer in full scan mode over a range of 300–1,600 m/z at a resolution r = 60,000. MS/MS data were acquired by isolating the 20 most intense ions, exhibiting charge states ≥2. Subsequently, they were subjected to fragmentation in the high-pressure linear ion trap by CID (collision-induced dissociation) with a normalized collision energy of 35%. Dynamic exclusion was enabled with the following setting: (a) exclusion size list of 500 peptides; (b) exclusion duration of 60; and (c) a repeat count of 1. An activation Q = 0.25 and an activation time of 10 ms were used.

2.4 Data analysis

Raw data were processed using MaxQuant v1.3.0.3 (Cox & Mann, 2008), and MS/MS spectra were searched against The Human UniProt database (released January 7, 2015, containing 93,275 sequences, and 37,039,836 residues) using the Andromeda search engine.

As search parameters, a tolerance of 6 ppm was considered for precursor ions (MS search) and 0.5 Da for fragment ions (MS/MS search), with a maximum of two missed cleavages. Carbamidomethylation of cysteine was considered a fixed modification, and oxidation of methionine and protein N-terminal acetylation were considered variable modifications.

A threshold of 1% of the false discovery rate (FDR) was set for both the protein and peptide identification. Protein quantification was performed using the LFQ algorithm implemented in MaxQuant software, with a minimum ratio count of 1 and a window of 2 min for matching between runs. Statistical analysis was performed with Perseus v1.5.2.6 software, which is available in the MaxQuant package. Identified protein entries were processed, excluding reverse sequences and those identified "only by site" entries. Keratins proteins identified in our study were not considered contaminants, as they are known to be expressed in our type of samples.

Protein abundance, which was calculated based on the normalized spectrum intensity (LFQ intensity), was log2-transformed, and the dataset was filtered by minimum valid values in at least one group (three valid values for at least one group). Significance was assessed using Student's *t* test to identify differentially expressed proteins between the OKC and normal oral mucosa ($p < .05$).

2.5 Functional enrichment analysis

For a system-wide understanding of cellular function, we used StringApp, which is an application designed to serve as a bridge between two well-known and widely used resources. We also used the STRING database (Szklarczyk et al., 2017) for quality-controlled protein–protein association networks and the Cytoscape software (Shannon, 2003) platform for network data integration.

From the proteomic analyses, the protein-coding genes were classified in two different categories: (a) Exclusive from OKC; (b) Significant differentially expressed (*p*-value < .05; log2 fold change ≥ 1.5). We used every ID given for each protein as a multiple "protein name" query for String App—restricted to those found on *Homo sapiens*. With this query STRING database collect and integrate data for those proteins, by consolidating known and predicted protein–protein association data for a large number of organisms based on: (a) systematic co-expression analysis, (b) detection of shared selective signals across genomes, (c) automated text-mining of the scientific literature, and (d) computational transfer of interaction knowledge between organisms based on gene orthology. For each protein–protein association stored in STRING, a score is provided. These scores (i.e., the "edge weights" in each network) represent confidence scores and are scaled between zero and one. They indicate the estimated likelihood that a given interaction is biologically meaningful, specific, and reproducible, given the supporting evidence (Szklarczyk et al., 2017). In this study, we used the default confidence score of 0.4.

With the output of a protein–protein interaction network, we then performed a functional enrichment analyses using the "retrieve functional analysis" tool on String App itself for each of the two categories generated. The enrichment tests were done for a variety of classification systems (Gene Ontology, KEGG, Pfam and InterPro, Reactome) and employ a Fisher's exact test followed by a correction for multiple testing—we used the default cutoff of 0.05.

One network was built for each established category. The networks retrieved came associated with a large number of node attributes for each protein and edge attributes for each interaction. From the IDs list, due to protein name ambiguity, our number of query Ids was about 3–5 times larger. However, this was normalized with STRING's disambiguation service to map the query proteins to the internal STRING identifiers database, and the exact query term that matched each protein is stored as a node attribute in the resulting STRING network in Cytoscape.

We manually evaluated all pathways and selected a non-overlapping set related to cell differentiation and tissue architecture. We selected pathways containing the terms: *differentiation*, *cell adhesion*, *cell attachment*, *cell junction*, *desmosome*, *cytoskeleton*, *keratin*, *intermediate filament*, extracellular matrix (ECM), *integrin, cadherin,* and *collagen*. Pathways containing terms associated with basal membrane and its components were not found.

2.6 Immunohistochemical data search

We searched in the literature for OKC immunohistochemical expression pattern of all the proteins identified in the selected enriched pathways of our study (Table 2).

3 RESULTS

We identified 1,150 proteins, of which 1,091 (95%) were expressed in both OKC and normal oral mucosa tissues (Figure 1; Table S1). One hundred sixty-four proteins were differently expressed ($p < .05$) (Table S2), and 72 showed a log2 fold change ≥ 1.5 (Figure 1). Twenty-seven proteins were exclusively found in the OKC group and in at least three OKC samples (Figure 1; Table 1).
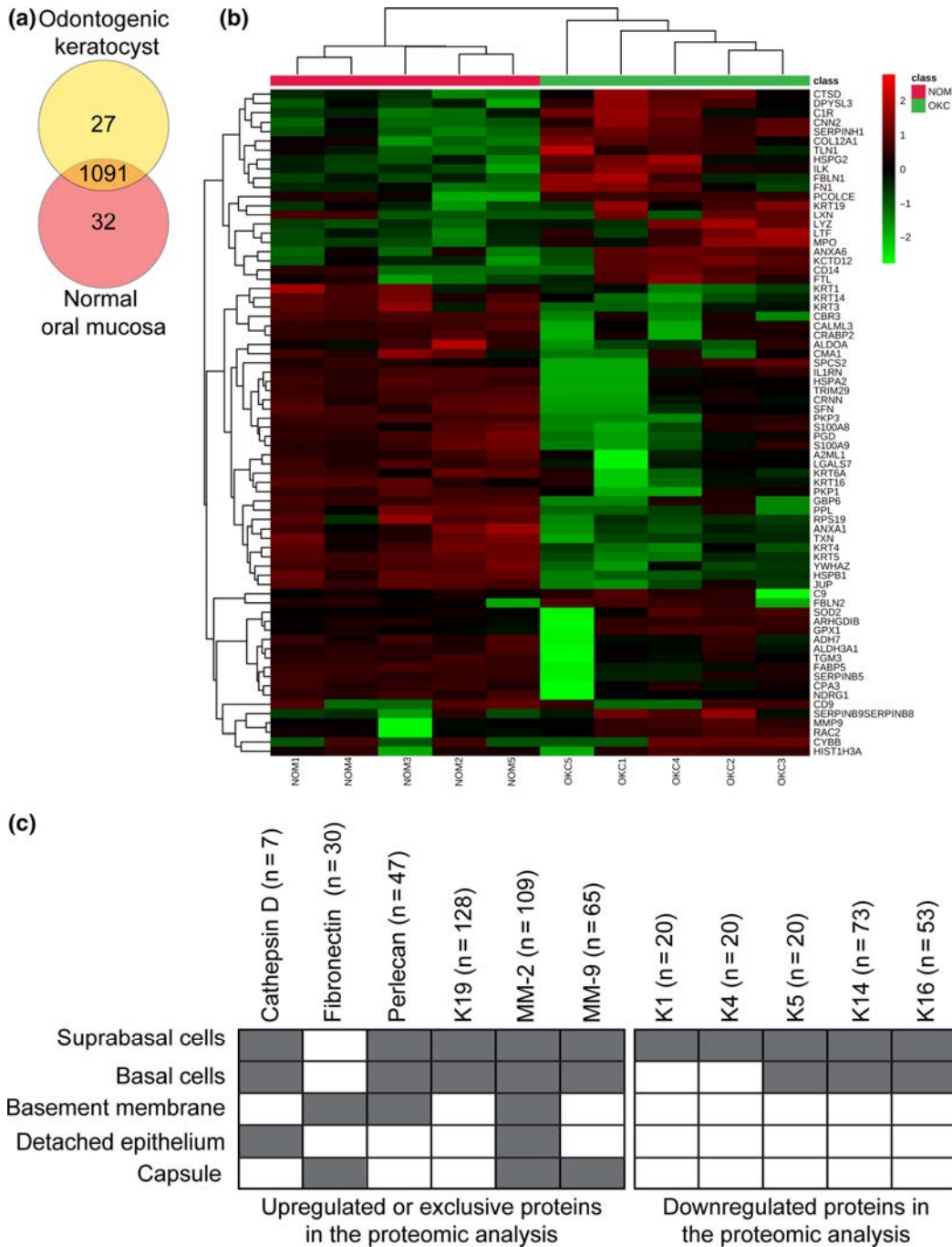
Figure 1. Proteomic analysis. The Venn diagram shows the relationship among sets of expressed proteins found in odontogenic keratocyst and normal oral mucosa (a) Heatmap displaying the expression of differentially expressed proteins ($p < .05$; log2 fold change ≥ 1.5) identified from the proteomics analysis. The heatmap was constructed in MetaboAnalyst 4.0 using the log2 transformed LFQ intensity of these proteins. The dendrograms were built using the following parameters: Euclidean distance and complete-linkage. The intensity of each protein is indicated by the color code, ranging from low (−2: green) to high (2: red) levels (b) The immunohistochemical expression of the targets identified in the proteomic enrichment analysis was retrieved from the literature and immunohistochemical studies of 11 proteins were found. The total number of samples investigated for each target is between parenthesis. All the immunohistochemical studies and details of the immunostaining are detailed in Table S5 (c) OKC, odontogenic keratotcyst; NOM, normal oral mucosa

Table 1. Proteins exclusively found in odontogenic keratocyst compared to matched oral normal mucosa

PROTEIN IDS	PROTEIN	GENE
Q9NRP0-2;Q9NRP0;A0A087WUD3	Oligosaccharyltransferase complex subunit OSTC	*OSTC*
A0A087WZM2;O00584;D6RHI9;D6REQ6;H0YAE9	Ribonuclease T2	*RNASET2*
A0A0G2JMH6;P01903;A0A0G2JH46;Q30118;A0A140TA34;P01906;Q5Y7H0;Q08AS3;A0A1W2PP70	HLA class II histocompatibility antigen, DR alpha chain/HLA class II histocompatibility antigen, DQ alpha 2 chain/HLA class II histocompatibility antigen DQ alpha chain	*HLA-DRA/HLA-DQA2/HLA-DQA1*
P08397;P08397-2;F5H345;P08397-3;P08397-4	Porphobilinogen deaminase	*HMBS*
P02786;G3V0E5	Transferrin receptor protein 1	*TFRC*
Q14767;G3V3X5;G3V511	Latent-transforming growth factor beta-binding protein 2	*LTBP2*
J3KNB4;P49913	Cathelicidin antimicrobial peptide	*CAMP*
P32322-3;P32322;P32322-2;J3KQ22;J3QKT4;J3QL24	Pyrroline-5-carboxylate reductase 1, mitochondrial	*PYCR1*
Q9UBT2;K7EPL2;K7ES38;U3KQ55	SUMO-activating enzyme subunit 2	*UBA2*
R4GMU1;O95479	GDH/6PGL endoplasmic bifunctional protein	*H6PD*
P02462	Collagen alpha-1(IV) chain;Arresten	*COL4A1*
P07711;Q5T8F0	Cathepsin L1	*CTSL*
P08240;P08240-2	Signal recognition particle receptor subunit alpha	*SRPRA*
P08253;P08253-3;P08253-2;H3BS34;H3BR66;H3BV48	72 kDa type IV collagenase (Matrix metalloproteinase-2) (MMP-2)	*MMP2*
P09467	Fructose-1,6-bisphosphatase 1	*FBP1*
P11215-2;P11215	Integrin alpha-M	*ITGAM*
P41091;Q2VIR3	Eukaryotic translation initiation factor 2 subunit 3/Eukaryotic translation initiation factor 2 subunit 3B	*EIF2S3/EIF2S3B*
X6R8F3;P80188;P80188-2	Neutrophil gelatinase-associated lipocalin	*LCN2*
Q07954	Prolow-density lipoprotein receptor-related protein 1	*LRP1*

Q12805;Q12805-3;Q12805-4;Q12805-2;Q12805-5;A0A0U1RQV3;Q580Q6;C9JPZ9;C9J4J8;C9JQX7	EGF-containing fibulin-like extracellular matrix protein 1 (Fibulin-3)	*EFEMP1*
Q15437;Q5QPE2	Protein transport protein Sec23B	*SEC23B*
Q16222;Q16222-3;Q16222-2	UDP-N-acetylhexosamine pyrophosphorylase	*UAP1*
Q6ZMP0;Q6ZMP0-4	Thrombospondin type-1 domain-containing protein 4	*THSD4*
Q7Z4H8;Q7Z4H8-2;Q7Z4H8-3;H0YEM3	Protein O-glucosyltransferase 3	*POGLUT3*
Q8TF66-2;Q8TF66	Leucine-rich repeat-containing protein 15	*LRRC15*
Q9UBR2	Cathepsin Z	*CTSZ*
Q9UQP3;A0A087WXC4;A0A087WXT0	Tenascin-N	*TNN*

The functional enrichment analysis was performed on the 72 differently expressed proteins with a log2 fold change ≥ 1.5 (Table S3) and on the 27 exclusive proteins (Table S4) separately. The enriched pathways were manually evaluated, and pathways related to cell differentiation and tissue architecture were selected (Figure 2). All the annotated proteins identified in the selected enriched pathways are listed in Table 2.

Figure 2. Enrichment analysis of proteomic data. Twenty-six pathways related to cell differentiation and tissue architecture were selected from the functional enrichment analysis of differentially expressed proteins in odontogenic keratocyst compared to normal oral mucosa ($p < .05$; log2 fold change ≥ 1.5) (a) Nine pathways related to tissue architecture and none related to cell differentiation were found in the enrichment analysis of proteins exclusively found in odontogenic keratocyst (b) ECM, extracellular matrix

Table 2. Target proteins in the enriched pathways related to cell differentiation and tissue architecture

PROTEIN	GENE	LOG2 FOLD CHANGE (OKC/NOM)
FRUCTOSE-BISPHOSPHATE ALDOLASE A	ALDOA	−1.62
ANNEXIN A1	ANXA1	−2.70
RHO GDP-DISSOCIATION INHIBITOR 2	ARHGDIB	1.55
CD9 ANTIGEN	CD9	−2.03
CHYMASE	CMA1	−1.91
CALPONIN-2	CNN2	2.88
COLLAGEN ALPHA-1(XII) CHAIN	COL12A1	2.93
CORNULIN	CRNN	−5.02
CATHEPSIN D	CTSD	1.53
DIHYDROPYRIMIDINASE-RELATED PROTEIN 3	DPYSL3	1.79
FIBULIN-1	FBLN1	3.34
FIBULIN-2	FBLN2	2.13
FIBRONECTIN	FN1	2.22
GLUTATHIONE PEROXIDASE 1	GPX1	2.40
HEAT SHOCK-RELATED 70 KDA PROTEIN 2	HSPA2	−3.18
HEAT SHOCK PROTEIN BETA-1	HSPB1	−2.98
BASEMENT MEMBRANE-SPECIFIC HEPARAN SULFATE PROTEOGLYCAN CORE PROTEIN (PERLECAN)	HSPG2	2.07
INTERLEUKIN-1 RECEPTOR ANTAGONIST PROTEIN	IL1RN	−2.19
INTEGRIN-LINKED PROTEIN KINASE	ILK	1.83
JUNCTION PLAKOGLOBIN	JUP	−3,42
KERATIN, TYPE II CYTOSKELETAL 1 (K1)	KRT1	−3.91
KERATIN, TYPE I CYTOSKELETAL 14 (K14)	KRT14	−2.95
KERATIN, TYPE I CYTOSKELETAL 16 (K16)	KRT16	−2.86
KERATIN, TYPE I CYTOSKELETAL 19 (K19)	KRT19	1.59
KERATIN, TYPE II CYTOSKELETAL 3 (K3)	KRT3	−4.29
KERATIN, TYPE II CYTOSKELETAL 4 (K4)	KRT4	−6.18
KERATIN, TYPE II CYTOSKELETAL 5 (K5)	KRT5	−2.95
KERATIN, TYPE II CYTOSKELETAL 6A (K6A)	KRT6A	−2.10
GALECTIN-7	LGALS7	−4.27
MATRIX METALLOPROTEINASE-9 (MMP-9)	MMP9	2.14
PROTEIN NDRG1	NDRG1	−2.05
PROCOLLAGEN C-ENDOPEPTIDASE ENHANCER 1	PCOLCE	1.53
PLAKOPHILIN-1	PKP1	−3.37
PLAKOPHILIN-3	PKP3	−2.09
PERIPLAKIN	PPL	−2.77
RAS-RELATED C3 BOTULINUM TOXIN SUBSTRATE 2	RAC2	2.05
PROTEIN S100-A8	S100A8	−1.70
PROTEIN S100-A9	S100A9	−2.07
SERPIN B5	SERPINB8	−1.92
SERPIN H1	SERPINH1	2.75
14-3-3 PROTEIN SIGMA	SFN/YWHAS	−3.07
PROTEIN-GLUTAMINE GAMMA-GLUTAMYLTRANSFERASE E	TGM3	−1.85
TALIN-1	TLN1	2.24
COLLAGEN ALPHA-1(IV) CHAIN;ARRESTEN	COL4A1	Exclusive in OKC
CATHEPSIN Z	CTSL	Exclusive in OKC
EGF-CONTAINING FIBULIN-LIKE EXTRACELLULAR MATRIX PROTEIN 1 (FIBULIN-3)	EFEMP1	Exclusive in OKC
INTEGRIN ALPHA-M	ITGAM	Exclusive in OKC
LATENT-TRANSFORMING GROWTH FACTOR BETA-BINDING PROTEIN 2	LTBP2	Exclusive in OKC
72 KDA TYPE IV COLLAGENASE (MATRIX METALLOPROTEINASE-2) (MMP-2)	MMP2	Exclusive in OKC
TENASCIN-N	TNN	Exclusive in OKC

Abbreviations: NOM, normal oral mucosa; OKC, odontogenic keraotcyst.

We searched the literature for immunohistochemical data of all annotated proteins presented in the selected enriched pathways and found the immunoexpression of 11 targets in OKC tissue, including proteases (Cathepsin D, MMP-2, MMP-9), ECM proteins (Fibronectin, Perlecan), and keratins (K1, K4, K5, K14, K16) (Table S5). The immunoexpression pattern

of the 11 targets according to previous OKC immunohistochemical studies are summarized in Figure 1.

A schematic illustration showing the OKC molecular architecture displaying the location and fold-regulation of the proteins found in our proteomic analysis is shown in Figure 3. The schema shows downregulation of the desmosomal proteins Junction plakoglobin (*JUP*), Plakophilin-1 (*PKP1*), Plakophilin-3 (*PKP3*) and Periplakin (*PPL*) and upregulation of proteases associated with ECM degradation, such as MMP-2, MMP-9, and Cathepsin D.
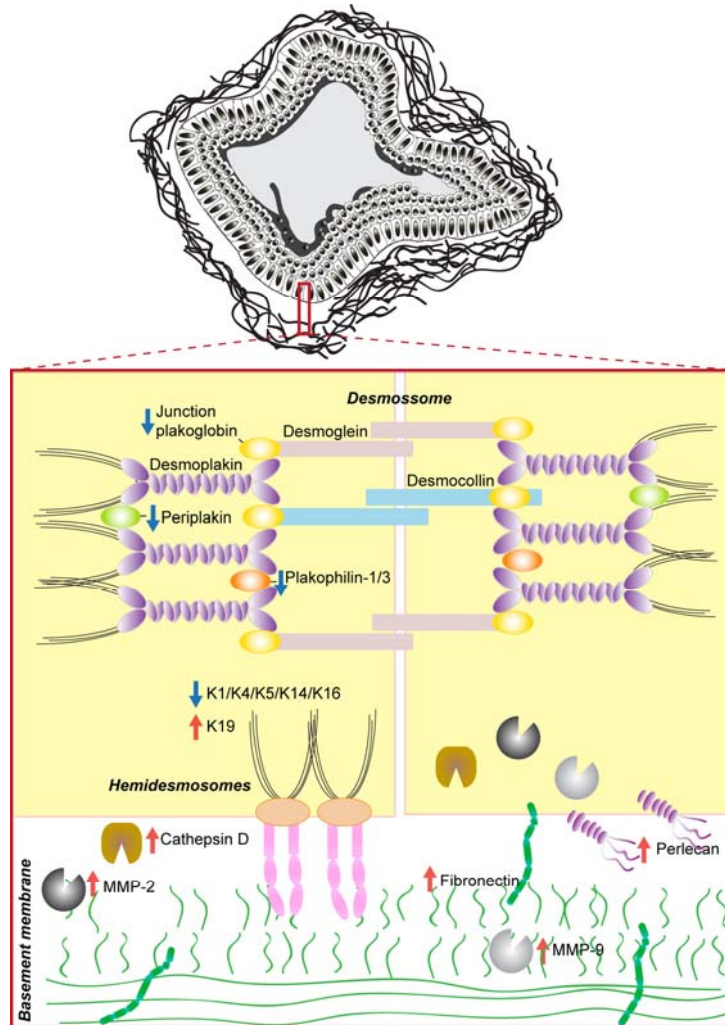

Figure 3. Schematic illustration of odontogenic keratocyst molecular architecture according to the proteomic analysis. The parakeratinized epithelium and separation of the epithelial lining from the underlying connective tissue wall of odontogenic keratocyst (OKC) are illustrated in the upper part of the figure. In the bottom are cell adhesion structures and extracellular matrix (ECM) components. Epithelial cells are joined together by many desmosome intercellular junctions formed by desmosomal proteins, of which cytoplasmic adapter proteins (Junction plakoglobin, *JUP*) and plaque-associated proteins (Plakophilin-1, *PKP1,* Plakophilin-3, *PKP3*, Periplakin *PPL*) are downregulated in OKC. Tonofilaments (keratins) end up inserting in the cytoplasmic thickening of the demosomes and hemidesmosomes and form cytoskeletal networks. Lysosomal cathepsins and matrix metaloproeinases (MMPs) are important players in ECM space. MMP-2 and MMP-9 cleave basement membrane collagen, while secreted cathepsins degrade collagen and other ECM proteins. MMP-2 and Cathepsin D are localized at the region of separation of epithelium from capsule. Other ECM components upregulated in OKC includes Fibronectin and Perlecan. Red arrows indicate positive fold-regulation and blue, negative, according to our comparative proteomic analysis

11

4 DISCUSSION

In the present study, we investigated the proteomic profile of OKC using LC-MS/MS method. In 2015, Malčić et al. reported a comparative proteomic profiling of OKC, oral mucosa, and radicular cyst using LC-MS/MS, but focusing on identifying potential biomarkers (Ivanišević Malčić et al., 2015). Fold-calculation and downregulated proteins were not provided. From the 43 proteins Malčić and colleagues identified in OKC comparing to oral mucosa, two are also in our list of upregulated differentially expressed proteins: procollagen C-endopeptidase enhancer (*PCOLCE*) and myeloperoxidase (*MPO*). Such differences in results can be explained by differences in protein extraction methods and/or data analysis.

Enrichment analysis provides valuable insights into the collective biological function underlying the list of differentially expressed proteins. In our study, we focused on pathways related to cell differentiation and tissue architecture to find targets associated with the pathobiology of OKC cells. In our enrichment analysis, we observed many pathways related to keratinocyte differentiation and cell adhesion structures, such as hemidesmosome and desmosome. Notably, compared to ameloblastoma, the OKC transcriptome analysis showed overexpression of genes associated with squamous epithelial differentiation and desmosome (Heikinheimo et al., 2015). Indeed, by histological and ultrastructural evaluation, the epithelial lining of OKC was shown to exhibit tall columnar basal cells showing cellular organelles, tonofilaments (keratins), hemidesmosomes, and desmosomes similar to basal cells of typical keratinizing squamous epithelium (Philipsen, Fejerskov, Donatsky, & Hjörting-Hansen, 1976). Many prominent desmosomes are observed at x1000 magnification in hematoxylin-eosin sections of OKC, and they are more frequently observed in OKC than in dentigerous and radicular cysts (Raju, Wadhwan, & Chaudhary, 2014). However, scanning electron microscopy analysis showed that these desmosomes were fragile and damaged at many places (Raju et al., 2014). Our analysis showed for the first time the downregulation of four proteins that form desmosomes: Junction plakoglobin (*JUP*), Plakophilin-1 (*PKP1*), Plakophilin-3 (*PKP3*), and Periplakin (*PPL*) (Figure 3). A plausible hypothesis is that the reduction of desmosomal proteins would lead to the fragile desmosomes previously observed by electron microscopy and could be associated with the fragile OKC epithelial lining associated with lesion recurrence after surgical treatment.

Our analysis also showed enriched pathways related to keratinization, pointing to a possible deregulation in proteins that participate in this process. In addition to desmosomes, keratin filaments play an important role in maintaining cohesion between epithelial cells and participate in the regulation of cell growth and migration (Etienne-Manneville, 2018). We found upregulation of K19 and downregulation of K1, K14, K16, K3, K4, K5, and K6A. Immunoexpression of K19, K1, K4, K5, K14, K16 in OKC epithelium was previously reported. Particularly, K19 expression is observed in odontogenic epithelium and in the epithelium of OKC and dentigerous cysts, but not in the epithelial lining of nasopalatine and epidermoid cysts, suggesting that K19 is a marker for odontogenic-derived cysts (Gao et al., 1989). In normal epithelium, the expression of KI9 was reported in non-keratinized oral tissues (i.e., buccal epithelium and in junctional, sulcular, and alveolar epithelium in gingiva) but not in the epidermis and keratinized oral tissues (Presland & Dale, 2000). Interestingly, OKC expresses K19, whereas the parakeratinized oral mucosa does not. The OKC parakeratin is unique among the jaw cysts. Whether the expression patterns of keratins are associated with OKC pathogenesis still needs to be clarified.

Besides pathways related to keratinocyte differentiation, keratinization, and desmosome, we found pathways of ECM organization and degradation. Separation of the epithelial lining from the underlying connective tissue cystic wall is frequently observed in OKC (Wilson & Ross, 1978), but not in other odontogenic cysts. This "weak" attachment between the epithelium and the cystic wall, upon removal, might leave reminiscent cells that can cause recurrence. The lack of rete ridges observed in OKC epithelial lining might be associated with the "weak" attachment. However, the separation of the epithelium from the supporting connective tissue of the cyst is suggested to be caused by metalloproteinases-mediated degradation of collagen in the juxtaepithelial regions (Khalifa, Shokier, & Abo-Hager, 2010; de Oliveira Ramos, Costa, Meurer, Vieira, & Rivero, 2014), which is supported by our results. We found upregulation of the metalloproteinases MMP-2 and MMP-9 in the OKC compared to matched normal oral mucosa. Additionally, previous studies reported intense immunoexpression of these MMPs in the epithelium, as well as in the connective tissue capsule. Noteworthy, MMP-2 was previously detected in the basement membrane zone of the detached OKC epithelium (Khalifa et al., 2010; Wahlgren et al., 2003) (Figure 3). We also found upregulation of cathepsin proteases from groups D, L, Z in our proteomic analysis. In line with our results, it was previously reported Cathepsin D immunoexpression at the region of separation of epithelium from connective tissue in 6/7 OKCs (Lakkasetty et al., 2015) (Figure 3). Collectively, these results suggest that MMPs and cathepsins might play a role in the separation of the epithelium from the supporting connective tissue in OKC, increasing the risk of recurrence.

Other ECM components are upregulated in OKC. These ECM components include fibronectin, which is expressed in the basement membrane and in the cystic capsule (De Oliveira, De Miranda, De Amorim, De Souza, & De & Almeida Freitas, 2004; Poomsawat, Punyasingh, & Weerapradist, 2006), and Perlecan, observed between intercellular bridges (Tsuneki et al., 2008, 2010; Wahba, Raghib, Megahed, & Hussein, 2013) (Figure 3). Fibronectin expression has been suggested to be related to OKC aggressive behavior (Poomsawat et al., 2006), while Perlecan expression was suggested as important for OKC proliferative potential (Tsuneki et al., 2008, 2010). Functional studies of these ECM molecules are necessary to clarify their role in OKC pathobiology.

In conclusion, our comparative proteomic analysis revealed pathways associated with keratinocyte differentiation, strengthening the notion that OKC cells have a similar proteomic profile to normal oral keratinocyte. Contextual investigation of the differentially expressed proteins revealed deregulation of desmosome proteins and ECM degradation as important alterations in OKC pathobiology. More molecular studies are needed to understand the molecular pathogenesiss of OKC, shedding light on the debate about the cystic or neoplastic nature of this odontogenic lesion.

ACKNOWLEDGEMENTS

CONFLICT OF INTEREST

None to declare.

AUTHOR CONTRIBUTIONS

Marina Gonçalves Diniz: Conceptualization; Data curation; Formal analysis; Investigation; Methodology; Supervision; Writing-original draft; Writing-review & editing. **Filipe Fideles Duarte-Andrade:** Data curation; Formal analysis; Methodology; Writing-review & editing. **Fernanda Stussi:** Formal analysis; Investigation; Methodology; Writing-review & editing. **Jessica Vitório:** Investigation; Methodology; Writing-review & editing. **Felipe Paiva Fonseca:** Investigation; Methodology; Writing-review & editing. **Romênia Ramos Domingues:** Data curation; Formal analysis; Investigation; Writing-review & editing. **Adriana Franco Paes Leme:** Data curation; Formal analysis; Resources; Writing-review & editing. **Carolina Cavalieri Gomes:** Conceptualization; Writing-original draft; Writing-review & editing. **Ricardo Santiago Gomez:** Conceptualization; Resources; Writing-original draft; Writing-review & editing.

REFERENCES

Barnes, L., Eveson, J. W., Reichard, P., & Sidransky, D. (Eds.) (2005). World Health Organization classification of tumours. Pathology and genetics of head and neck tumours, 3rd ed. Lyon, France: IARC Press.

Cox, J., & Mann, M. (2008). MaxQuant enables high peptide identification rates, individualized p.p.b.-range mass accuracies and proteome-wide protein quantification. *Nature Biotechnology*, 26, 1367– 1372. https://doi.org/10.1038/nbt.1511

de Oliveira, M. D. C., De Miranda, J. L., De Amorim, R. F. B., De Souza, L. B., & & De Almeida Freitas, R. (2004). Tenascin and fibronectin expression in odontogenic cysts. *Journal of Oral Pathology and Medicine*, 33, 354– 359. https://doi.org/10.1111/j.1600-0714.2004.00212.x

de Oliveira Ramos, G., Costa, A., Meurer, M. I., Vieira, D. S. C., & Rivero, E. R. C. (2014). Immunohistochemical analysis of matrix metalloproteinases (1, 2, and 9), Ki-67, and myofibroblasts in keratocystic odontogenic tumors and pericoronal follicles. *Journal of Oral Pathology and Medicine*, 43, 282– 288. https://doi.org/10.1111/jop.12131

Diniz, M. G., Galvão, C. F., Macedo, P. S., Gomes, C. C., & Gomez, R. S. (2011). Evidence of loss of heterozygosity of the PTCH gene in orthokeratinized odontogenic cyst. *Journal of Oral Pathology and Medicine*, 40, 277– 280. https://doi.org/10.1111/j.1600-0714.2010.00977.x

El-Naggar, A. K., Chan, J. K. C., Grandis, J. R., Takata, T., & Slootweg, P. J. (Eds.) (2017). WHO Classification of head and neck tumours, 4th ed. Lyon, France: IARC Press.

Etienne-Manneville, S. (2018). Cytoplasmic intermediate filaments in cell biology. *Annual Review of Cell and Developmental Biology*, 34, 1– 28. https://doi.org/10.1146/annurev-cellbio-100617-062534

Gao, Z., Mackenzie, I. C., Cruchley, A. T., Williams, D. M., Leigh, I., & Lane, E. B. (1989). Cytokeratin expression of the odontogenic epithelia in dental follicles and developmental cysts. *Journal of Oral Pathology and Medicine*, 18, 63– 67. https://doi.org/10.1111/j.1600-0714.1989.tb00738.x

Gomes, C. C., Guimarães, L. M., Diniz, M. G., & Gomez, R. S. (2017). Molecular alterations in odontogenic keratocysts as potential therapeutic targets. *Journal of Oral Pathology and Medicine*, 46, 877– 882. https://doi.org/10.1111/jop.12591

Heikinheimo, K., Kurppa, K. J., Laiho, A., Peltonen, S., Berdal, A., Bouattour, A., … Morgan, P. R. (2015). Early dental epithelial transcription factors distinguish ameloblastoma from keratocystic odontogenic tumor. *Journal of Dental Research*, 94, 101– 111. https://doi.org/10.1177/0022034514556815

Ide, F., Kikuchi, K., Miyazaki, Y., Mishima, K., Saito, I., & Kusama, K. (2010). Keratocyst of the buccal mucosa: Is it odontogenic? *Oral Surgery, Oral Medicine, Oral Pathology, Oral Radiology, and Endodontology*, 110, e42– e47. https://doi.org/10.1016/j.tripleo.2010.05.073

Ivanišević Malčić, A., Breen, L., Josić, D., Jukić Krmek, S., Džombeta, T., Matijević, J., … Kraljević Pavelić, S. (2015). Proteomics profiling of keratocystic odontogenic tumours reveals AIDA as novel biomarker candidate. *Journal of Oral Pathology and Medicine*, 44, 367– 377. https://doi.org/10.1111/jop.12239

Khalifa, G. A., Shokier, H. M., & Abo-Hager, E. A. (2010). Evaluation of neoplastic nature of keratocystic odontogenic tumor versus ameloblastoma. *Journal of the Egyptian National Cancer Institute*, 22, 61– 72.

Lakkasetty, Y., Venkatraman, N., Balasundari, S., Shashidara, R., Leeky, M., & Shivamalappa, S. M. (2015). The expression of cathepsin-D in odontogenic cysts and tumors: Immunohistochemistry study. *Journal of Advanced Clinical & Research Insights*, 2, 67– 71. https://doi.org/10.15713/ins.jcri.47

Odell, E. (2017). Cawson's essentials of oral pathology and oral medicine, 9th ed. Amsterdam, Netherlands: Elsevier.

Pavelić, B., Levanat, S., Crnić, I., Kobler, P., Anić, I., Manojlović, S., & Sutalo, J. (2001). PTCH gene altered in dentigerous cysts. *Journal of Oral Pathology and Medicine*, 30, 569– 576. https://doi.org/10.1034/j.1600-0714.2001.300911.x

Philipsen, H. P., Fejerskov, O., Donatsky, O., & Hjörting-Hansen, E. (1976). Ultrastructure of epithelial lining of keratocysts in nevoid basal cell carcinoma syndrome. *International Journal of Oral Surgery*, 5, 71– 81. https://doi.org/10.1016/s0300-9785(76)80051-8

Poomsawat, S., Punyasingh, J., & Weerapradist, W. (2006). Expression of basement membrane components in odontogenic cysts. *Oral Diseases*, 12, 290– 296. https://doi.org/10.1111/j.1601-0825.2005.01193.x

Presland, R. B., & Dale, B. A. (2000). Epithelial structural proteins of the skin and oral cavity: Function in health and disease. *Critical Reviews in Oral Biology and Medicine*, 11, 383– 408. https://doi.org/10.1177/10454411000110040101

Qu, J., Zhang, J., Zhang, H., Li, X., Hong, Y., Zhai, J., … Li, T. (2019). PTCH1 alterations are frequent but other genetic alterations are rare in sporadic odontogenic keratocysts. *Oral Diseases*, 25, 1600– 1607. https://doi.org/10.1111/odi.13135

Raju, P., Wadhwan, V., & Chaudhary, M. (2014). Desmosomes: A light microscopic and ultrastructural analysis of desmosomes in odontogenic cysts. *Journal of Oral and Maxillofacial Pathology*, 18, 336. https://doi.org/10.4103/0973-029X.151309

Rappsilber, J., Mann, M., & Ishihama, Y. (2007). Protocol for micro-purification, enrichment, pre-fractionation and storage of peptides for proteomics using StageTips. *Nature Protocols*, 2, 1896– 1906. https://doi.org/10.1038/nprot.2007.261

Shannon, P. (2003). Cytoscape: A software environment for integrated models of biomolecular interaction networks. *Genome Research*, 13, 2498– 2504. https://doi.org/10.1101/gr.1239303

Szklarczyk, D., Morris, J. H., Cook, H., Kuhn, M., Wyder, S., Simonovic, M., … von Mering, C. (2017). The STRING database in 2017: Quality-controlled protein–protein association networks, made broadly accessible. *Nucleic Acids Research*, 45, D362– D368. https://doi.org/10.1093/nar/gkw937

Tsuneki, M., Cheng, J., Maruyama, S., Ida-Yonemochi, H., Nakajima, M., & Saku, T. (2008). Perlecan-rich epithelial linings as a background of proliferative potentials of keratocystic odontogenic tumor. *Journal of Oral Pathology and Medicine*, 37, 287– 293. https://doi.org/10.1111/j.1600-0714.2007.00620.x

Tsuneki, M., Yamazaki, M., Cheng, J., Maruyama, S., Kobayashi, T., & Saku, T. (2010). Combined immunohistochemistry for the differential diagnosis of cystic jaw lesions: Its practical use in surgical pathology. *Histopathology*, 57, 806– 813. https://doi.org/10.1111/j.1365-2559.2010.03712.x

Wahba, O. M., Raghib, A. M., Megahed, E. M., & Hussein, M. M. (2013). Expression of perlecan, syndecan-1 and Ki-67 in keratocystic odontogenic tumor. *Tanta Dental Journal*, 10, 153– 159. https://doi.org/10.1016/j.tdj.2013.12.003

Wahlgren, J., Vaananen, A., Teronen, O., Sorsa, T., Pirila, E., Hietanen, J., … Salo, T. (2003). Laminin-5 gamma 2 chain is colocalized with gelatinase-A (MMP-2) and collagenase-3 (MMP-13) in odontogenic keratocysts. *Journal of Oral Pathology and Medicine*, 32, 100– 107. https://doi.org/10.1034/j.1600-0714.2003.00075.x

Wilson, D. F., & Ross, A. S. (1978). Ultrastructure of odontogenic keratocysts. *Oral Surgery, Oral Medicine, Oral Pathology*, 45, 887– 893. https://doi.org/10.1016/s0030-4220(78)80011-5